



## FEI based Online Actuator Tracking Assessment for Real-Time Hybrid Simulation

Tong Guo<sup>1</sup>, Weijie Xu<sup>1</sup>, Cheng Chen<sup>2</sup>

1 Professor, Key Laboratory of Concrete and Prestressed Concrete Structures of the Ministry of Education, Southeast University, Nanjing, P.R. China. E-mail: Guotong77@gmail.com

2 PhD student, Key Laboratory of Concrete and Prestressed Concrete Structures of the Ministry of Education, Southeast University, Nanjing, P.R. China. E-mail: xwj19900429@gmail.com

3 Assistant Professor, School of Engineering, San Francisco State University, San Francisco, CA, USA. E-mail: chcsfsu@sfsu.edu

### ABSTRACT

Frequency-domain evaluation index (FEI) is a novel technical which can capture both the time delay and amplitude of the real-time hybrid simulation. However, the time delay and amplitude calculated by FEI are mean values. In this study, moving windows with overlap is investigated through computational simulations. Existing RTHS data from Network Earthquake Engineering Simulation (NEES) are further analyzed to evaluate the effectiveness of the proposed online approach. It is demonstrated that moving window technical enables accurate online actuator tracking for real-time hybrid simulation.

**KEYWORDS:** *real-time hybrid simulation, frequency-domain evaluation index, tracking error, moving window*

### 1. GENERAL INSTRUCTIONS

Real-time hybrid simulation (RTHS) allows researchers to observe the behavior of critical elements at large or full scale when subjected to dynamic loading [1-3]. Fig. 1.1 shows a typical process of the RTHS. Since the process is conducted in a real-time manner, RTHS provides an efficient and economical technique to account for rate-dependence of some seismic devices in size limited laboratories [4-5].

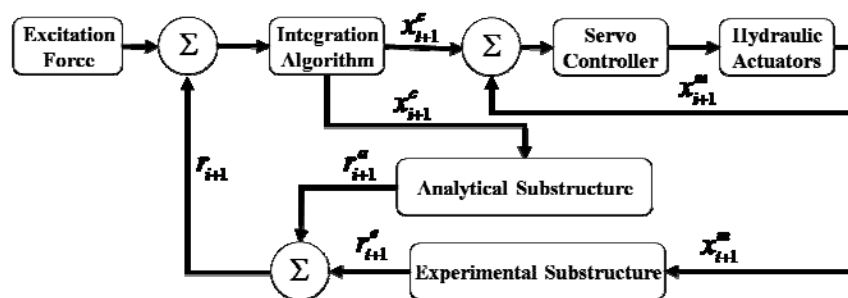


Figure 1.1 Typical process of real-time hybrid simulation

In RTHS, there are inevitable time delays, such as communication delay, computing time delay and actuator dynamics, resulting in the forces from the experimental substructures asynchronous with the calculated displacements. Various compensation methods have been proposed to avoid the instability caused by actuator delay and to improve actuator tracking. Experimental studies however showed that the test error can be reduced but cannot be completely eliminated even with sophisticated compensation methods [4]. Thus, actuator tracking evaluation becomes critical to ensure reliable experimental results for appropriate interpretation of structural performance under selected ground motions. Guo et al. [6] proposed a frequency evaluation index (FEI) method to evaluate the actuator tracking in terms of amplitude error and phase error. By the concept of equivalent frequency, the time delay of the test can be quantitatively calculated. The FEI method is shown to provide accuracy estimate of actuator delay even when for the experimental substructures in RTHS involve nonlinear structural behavior and rate-dependent elastomeric damper. More recently, Guo et al. [7] also proposed two decimate factors to improve

the calculation efficiency of the FEI. These findings show that the FEI method provides an innovative and effective way for post-test assessment of actuator tracking error.

For a typical seismic test, peak structural response often occurs within a short time window of 2 to 8 seconds, while the duration of the entire test could be as long as 60 seconds. Accurate actuator tracking during this short time window is more critical for replicating structural performance under earthquakes. Moreover, due to the cost of structural experiments, it is worthwhile to stop the test before the experimental specimen is damaged when actuator compensation is not properly determined. This requires an online assessment tool to identify actuator tracking error in a timely manner [8-9]. In this paper, the FEI based online actuator tracking assessment is developed through Short Time Fourier Transform. Moving windows with fixed data length are used to provide local quantitative error. Both computational simulations and laboratory tests are used to evaluate the effectiveness of the proposed FEI based method.

## 2. FREQUENCY-DOMAIN EVALUATION INDEX

The FEI provides an innovative way for quantitative post-simulation evaluation of actuator tracking errors, which can be written as,

$$FEI = \sum_{j=1}^p \left\{ \frac{y_o(f_i)}{y_i(f_i)} \cdot \frac{\|y_i(f_i)\|^2}{\sum_{i=1}^p \|y_i(f_i)\|^2} \right\} \quad (2.1)$$

$$A = \|FEI\| \quad (2.2)$$

$$\phi = \arctan[\text{Im}(FEI) / \text{Re}(FEI)] \quad (2.3)$$

$$f^{eq} = \frac{\sum_{i=0}^p (\|y_i(f_i)\|^2 \cdot f_i)}{\sum_{i=0}^p \|y_i(f_i)\|^2} \quad (2.4)$$

$$d = -\phi / (2\pi \cdot f^{eq}) \quad (2.5)$$

where  $y_i(f)$  and  $y_o(f)$  represent the FFT of the input and output signals, respectively.  $A$ ,  $\phi$ ,  $f^{eq}$  and  $d$  are generalized amplitude, phase equivalent frequency and equivalent delay, respectively; and  $p$  is the number of frequencies to be considered; and  $f_i$  is the  $i$ th frequency. According to FFT,  $2p$  equals to the smallest power of two that is greater than or equals to the number of data points. To eliminate the effect of the spectrum leakage [10], the mean of both input and output signals should be removed and a Hanning window is introduced before FFT. The closer that  $A$  is to 1 and  $d$  is to 0, the more accurately that the output signal replicating the input signal.

## 3. MOVING WINDOW TECHNIQUE

For signals with limited length, the Short Time Fourier Transform (STFT) can be expressed as,

$$X(t, f) = \int_{-\infty}^{+\infty} \omega(t - \tau) x(\tau) e^{-j2\pi f\tau} d\tau \quad (3.1)$$

where  $\omega(t)$  is window function to reduce the effect of spectrum leakage;  $x(\tau)$  and  $X(t, f)$  are the signal in the time domain and frequency domain, respectively. In this study, a Hanning window is used in the FEI, which can be written as,

$$\omega(t) = \begin{cases} \frac{1}{2(t_2 - t_1)} (1 + \cos \frac{\pi(t - t_1)}{t_2 - t_1}) & t_1 \leq t \leq t_2 \\ 0 & t < t_1, t_2 < t \end{cases} \quad (3.2)$$

where  $t_1$  and  $t_2$  are the start and the end time of the signal to be analyzed. According to Eq. (3.2), the window size  $t_w$  equals  $(t_2 - t_1)$ . The corresponding data length  $N$  equals the window size multiplies the sampling frequency. For the purpose of clarification, both the data length  $N$  and window size  $t_w$  refer to the same concept where the former represents the number of data points and the latter show the length of window in time. The moving windows are applied in two ways, namely moving window without overlapping (MW) and moving window with overlapping (MWO). The end time  $t_2$  is the start time  $t_1$  of the next window for windows without overlap, while the end time  $t_2$  is larger than the start time  $t_1$  of the next window for the windows with overlap, which are shown in Fig. 2.1.



Figure 2.1 Moving windows technical for (a) without overlap and (b) with overlap

One of the pitfalls of the STFT is that it has a fixed resolution. The width of the windowing function relates to how the signal is represented—it determines whether there is good frequency resolution (frequency components close together can be separated) or good time resolution (the time at which frequencies change). A wide window gives better frequency resolution but poor time resolution. A narrower window gives good time resolution but poor frequency resolution. These are called narrowband and wideband transforms, respectively.

#### 4. NUMERICAL SIMULATION

One of the most important factors that influence window size is frequency of the structure. To reveal the relationship between window size and frequency, numerical simulations for a single degree of freedom structure are conducted utilizing the block diagram in Fig. 4.1., where the transport delay block represents the constant time delay in actuator response while the gain block represents the amplitude error. Ten ground motions are randomly selected from the Pacific Earthquake Engineering Research (PEER) Strong Motion Database [11], and the sampling rate is taken as 1024 Hz. The mass of the structure is 1 kg, and the inherent viscous damping ratio of the SDOF structure is assumed to be 2%. To investigate the influence of natural frequency on the window size, the natural frequency of the structure varies from 0.2 Hz to 5.1 Hz with an interval of 0.1 Hz. The amplitude  $k_p$  and time delay  $\tau$  have constant values of 1 and 1 msec., respectively. The  $t_w$  for moving windows increases from the natural period of the structure with an increment of 0.1 times of natural period until the error between time delay calculated using the FEI and the theoretical value is less than 1% (i.e. 0.01msec.). The relationship between structure property and the desired  $t_w$  for linear structure can be seen in Fig.4.2.

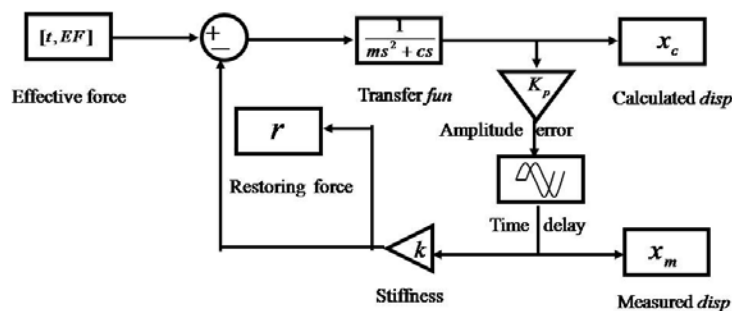


Figure 4.1 Block diagram representation for computational simulation

As can be observed from Fig.4.2, the window size to achieve good accuracy of the analysis results is affected by the natural frequency of the structure. For the same ground motion, the lower the natural frequency is, the larger the window size is necessary. For the same natural frequency/period, the window size varies for different ground motions to achieve good accuracy. It can also be observed that accurate results can be achieved when the window size is twice or three times of the natural period of the linear elastic structure. Good time resolution can be

achieved when the frequency of the structure is large, but the performance for low natural frequency is poor. To overcome this problem, the moving window with overlapping is investigated in this paper.

Assuming that the overlap length between two adjacent windows is  $OL$ , the MWO is the same as MW when  $OL$  equals 0. The larger the  $OL$  is, the more details the FEI will be calculated. Thus,  $OL$  should be selected to be the largest possible value as following

$$OL = N - 1 \quad (7)$$

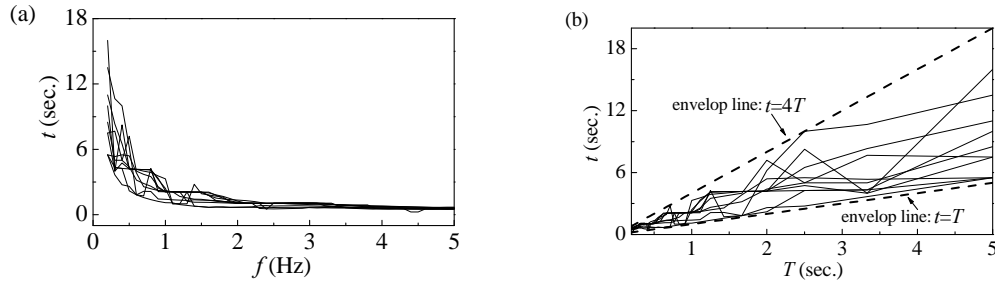


Figure 4.2 Relationship between structure properties and desired  $t_w$  for linear structure for (a) natural frequency and (b) fundamental period

To further verify the effectiveness of the proposed method, computational simulations are conducted for both linear and nonlinear structures. The BoucWen model [12] is used to emulate the restoring force for nonlinear structure as following:

$$r^a(t) = \eta \cdot k_a \cdot x^a(t) + (1 - \eta) \cdot k_a \cdot x_y^a \cdot z(t) \quad (4.1)$$

$$x_y^a \cdot \dot{z}(t) + \gamma |\dot{x}^a(t)| \cdot z(t) \cdot |z(t)|^{q-1} + \beta \cdot \dot{x}^a(t) \cdot |z(t)|^q - \dot{x}^a(t) = 0 \quad (4.2)$$

where  $x_y^a$  is the yield displacement and set to 10 mm;  $k_a$  is the linear elastic stiffness of the analytical substructure and is set to 11.765 kN/mm;  $\eta$  is the ratio of the post- to pre-yield stiffness of the analytical substructure and is set to 0;  $x_a(t)$  is the displacement imposed on the analytical substructure by the integration algorithm; and  $z(t)$  is the evolutionary parameter of the Bouc–Wen model and the dimensionless parameters  $\beta$ ,  $\gamma$ ,  $q$  control the shape of the hysteric loop of the analytical substructure, the values of the parameters are set to 0.55, 0.45 and 2, respectively.

For the purpose of demonstration, three fundamental frequency of the SDOF structure is selected as 1.0 Hz, which corresponds to the natural period 1 sec.. It should also be noted that similar results can also be observed for other frequencies. The time delay and amplitude error between calculated displacement and measured displacement are 5 msec. and 1.1, respectively. The CAP000 component recorded at Capitola station during the 1989 Loma Prieta earthquake is selected from the PEER Strong Motion Database with the peak ground acceleration of 0.0528g. The measured displacements for linear and nonlinear structure are presented in Fig.4.3, where the nonlinear structural behavior when the displacement response exceeds the yield displacement of 10 mm.

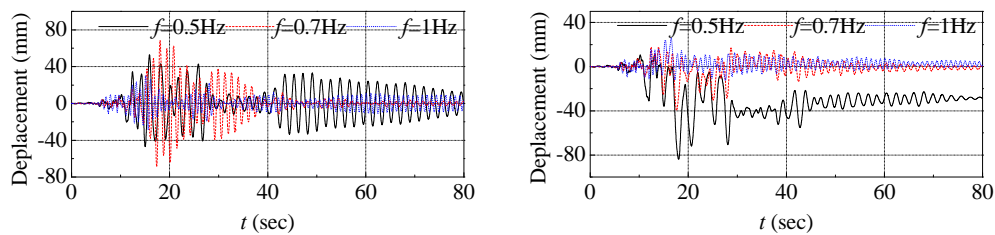


Figure 4.3 Measured displacements for (a) linear structures and (b) nonlinear structures

The analysis results using the moving window with overlap for different frequency structure are presented in g Fig. 4.4. As can be observed in Figs. 4.4(a) and 4.4 (c), the error between calculated and theoretical amplitudes is less

than 1%, which shows the advantages of the moving window with overlap. Meanwhile, it is observed that the analysis results for structure with high frequency are more accurate than those with low frequency. The similar conclusion can also be made in Figs. 4.4 (b) and 4.4(d). The relatively large oscillation in Fig. 4.4(d) when the frequency is 0.5 Hz is mainly due to the nonlinearity of the structure. The maximum errors of the calculated indexes using MWO technical are presented in Tab. 4.1.

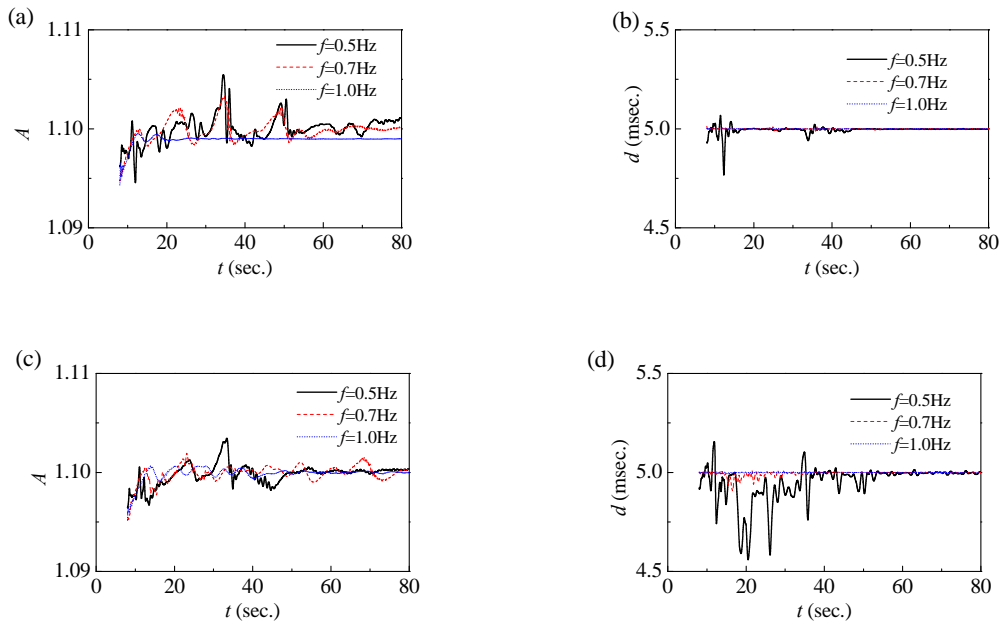


Figure 4.6 Analysis results for structural natural frequency of 1.0 Hz (a)  $A$  for linear structure; (b)  $d$  for linear structure; (c)  $A$  for nonlinear structure and (d)  $d$  for nonlinear structure

Table 4.1 Maximum error of the calculated indexes for different frequency (%)

Frequency	Linear structure		Nonlinear structure	
	$A$	$d$	$A$	$d$
0.5 Hz	0.5	1.4	0.3	8.8
0.7 Hz	0.5	0.3	0.4	1.8
1.0 Hz	0.6	0.1	0.4	0.2

It can be observed from Tab.4.3 that the maximum amplitude error for both linear structure and nonlinear structure varies from 0.3% to 0.6%, which means the moving window technical provides an accuracy estimates for amplitude. The maximum delay error for 0.5 Hz structure is the largest among three frequencies for both linear structure and nonlinear structure. Meanwhile, the performance for linear structure is much better than nonlinear structure for the same frequency.

## 5 EXPERIMENTAL VERIFICATION

Experimental data from project 711 in NEEShub [13] are analyzed to verify the effectiveness of the moving window in online evaluation. The analytical substructure is the SDOF MRF, which has a mass of 503.4 metric tons, an elastic natural frequency of 0.77 Hz, and an inherent viscous damping ratio of 0.02. The experimental substructure is an elastomeric damper. The restoring force of the SDOF MRF is emulated using the same Bouc-Wen model in Eq. (4.1) and Eq. (4.2). The N169E component of the 1994 Northridge earthquake recorded at Canoga Park was selected as the ground motion, and the maximum ground acceleration was scaled to  $0.322\text{m/s}^2$  to satisfy the limits imposed by the servo-hydraulic equipment. The unconditionally stable explicit CR integration algorithm was used for the real-time hybrid simulations. The inverse compensation method with different actuator delay estimates (15msec., 29msec. and 45msec.) was used to negate the effect of servo-hydraulic dynamics.

The amplitude  $A$  and equivalent delay  $d$  from frequency-domain evaluation of the three real-time hybrid simulations are presented in Tab. 5.1. The amplitude errors for all three tests are less than 0.5%, indicating the good tracking of the tests. The equivalent time delay is identified as 12.3 msec. when  $\alpha_{es}$  equals to 15,

demonstrating the measured displacement lags behind the calculated displacement about 12.3 msec.. When  $\alpha_{es}$  equals to 29, the equivalent delay is -1.1 msec., illustrating the measured displacements leads the calculated displacements about 1.1 msec.. When  $\alpha_{es}$  equals to 45, the equivalent delay is -16.2 msec., indicating the measured displacement leads the calculated displacements about 16.2 msec.. It can be concluded that the test with  $\alpha_{es}$  of 29 is most reliable among the three tests. Time histories of the calculated, command, and measured displacements are presented in Fig.5.1, which are identical with the analysis above. As the natural frequency of the analytical substructure is 0.77 Hz, the similar window size as numerical simulation is selected for each test. The analysis results are presented in Fig. 5.2.

Table 5.1 FEI analysis of Project 711 over duration of entire test

$\alpha_{es}$	A	d (msec.)
15	1.003	12.3
29	1.001	-1.1
45	1.005	-16.2

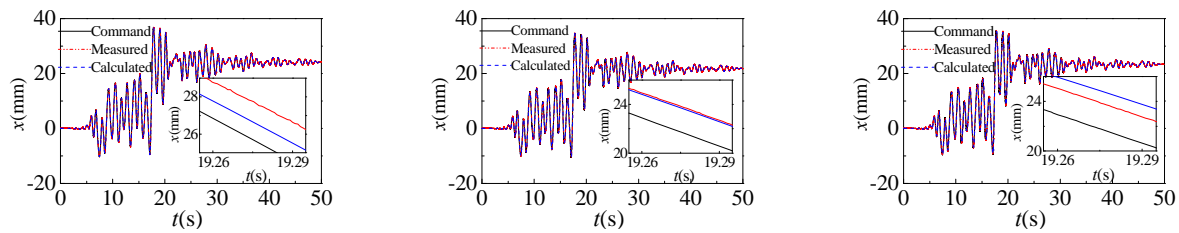


Figure 5.1 Comparison between calculated, command and measured displacements for project 711 for (a)  $\alpha_{es}=15$ ; (b)  $\alpha_{es}=29$  and (c)  $\alpha_{es}=45$ .

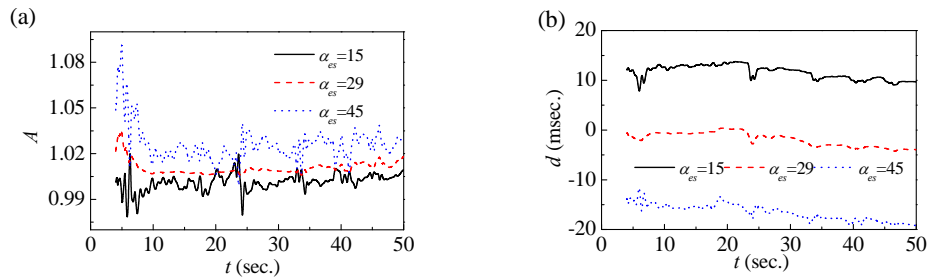


Figure 5.2 Online evaluation on the project 711 for (a)  $A$  and (b)  $d$

As can be observed from Fig. 5.2, the amplitude and time delay of the tests for every millisecond can be evaluated. In Fig. 5.2 (a), the amplitude for three tests all vary around 1.0, which indicates the good tracking of the test when the displacements are large. The time delay varies around 10 msec. when  $\alpha_{es}$  equals 15 in Fig. 5.2 (b). When  $\alpha_{es}$  equals 29, the time delay varies around -1 msec.. While  $\alpha_{es}$  equals 45, the time delay varies around -15 msec.. These conclusions are identical with Table 5.1.

## 6 SUMMARY AND CONCLUSION

Accurate evaluation of actuator tracking is detrimental to ensure the reliability of real-time hybrid simulation results. Though the FEI provides an effective way to evaluate the real-hybrid simulation in frequency domain, it has difficulties in evaluating the performance of the tests online. In this paper, moving window technical is proposed to overcome this problem. Computational simulations are conducted to determine the window length and verify the effectiveness of these methods. Existing real-time hybrid tests are utilized to demonstrate the effectiveness of the proposed approaches. Based on the assumptions and limitations of this paper, conclusions are drawn as follows. The required window size for moving window depends on the natural frequency and structural nonlinearity as well as the ground motion input. The larger natural period and stronger nonlinearity of the structure, the larger window length is required in localized evaluation. Moving window with overlap can be used to evaluate the local performance of the real-time hybrid simulation.

## ACKNOWLEDGEMENTS

The authors would like to acknowledge the support from National Science Foundation of China under grant No.51378107. The author would also like to acknowledge the support from the Fundamental Research Funds for the Central Universities and Priority Academic Program Development of Jiangsu Higher Education Institutions under the award number KYLX-0158 and Scientific Research Foundation of Graduate School of Southeast University.

## REFERENCES

1. Nakashima M., Kato H. and Takaoka E. (1992). Development of real-time pseudodynamic testing. *Earthquake Engineering and Structural Dynamics*. **21:1**,79-92.
2. Darby A.P., Blakeborough A. and Williams M.S. (1999). Real-time substructure tests using hydraulic actuators. *Journal of Engineering Mechanics*. **125:10**,1133-1139.
3. Blakeborough A., Williams M.S., Darby A.P., et al. (2001). The development of real-time substructure testing. *Philosophical Transactions of the Royal Society of London A*. **359**,1869-1891
4. Christenson R., Lin Y.Z., Emmons A. and Bass B. (2008). Large-scale experimental verification of semi-active control through real-time hybrid simulation. *Journal of Structural Engineering*. **134:4**,522-534.
5. Chen C., Ricles J.M., Karavasilis T., Chae Y., et al. (2012). Real-Time Hybrid Simulation System for Performance Evaluation of Structures with Rate Dependent Devices Subjected to Seismic Loading. *Engineering Structures*. **35**,71-82.
6. Guo T., Chen C., Xu W. J., et al. (2014). A frequency response analysis approach for quantitative assessment of actuator tracking for real-time hybrid simulation. *Smart Materials and Structures*. **23:4**, 045042.
7. Guo T., Xu W. J., Chen C.(2014). Analysis of Decimation Techniques to Improve Computational Efficiency of a Frequency-domain Evaluation Approach for Real-Time Hybrid Simulation. *Journal of Smart Structures and Systems*. **14:6**, 1197-1220.
8. Elkhoraibi T. and Mosalam K.M. (2012). Towards error - free hybrid simulation using mixed variables. *Earthquake engineering and structural dynamics*. **36:11**, 1497-1522.
9. Chen C. and Sharma R. (2012). A Reliability Assessment Approach for Real-Time Hybrid Simulation Results. *Canadian Society for Civil Engineering annual conference and 3rd International Structural Specialty Conference*, Edmonton, Alberta, Canada.
10. Bracewell R.N. (2000).The Fourier Transform and Its Applications. 3rd ed., Boston, McGraw-Hill.
11. PEER Strong Ground Motion Database. (2009). <http://peer.berkeley.edu>.
12. Wen Y.K. (1980). Equivalent linearization for hysteretic systems under random excitation. *Journal of Applied Mechanics*. **47:1**,150-154.
13. Ricles J.M. (2008). Advanced Servo-Hydraulic Control and Real-Time Testing of Damped Structures. <https://nees.org/warehouse/project/711>.